Sand Dust Image Enhancement and Infrared Strip Noise Removal Using Anisotropic Guided Filter

RPVG Ashok Reddy[1], T Umamaheswari[2], P Subbarayudu[3]

[1]**Assistant Professor**, *Department of ECE, KSRMCE, Kadapa, Andhra Pradesh.*

[2]**Assistant Professor**, *Department of ECE, KSRMCE, Kadapa, Andhra Pradesh.*

[3]**Assistant Professor**, *Department of ECE, KSRMCE, Kadapa, Andhra Pradesh.*

Abstract

The guided filter and its later variations have been widely used in various image processing and computer vision applications, owing to its minimal complexity and good edge-preservation features. Despite this success, the guided filter's various variations are unable to handle increasingly aggressive filtering strengths, resulting in the appearance of "detail halos." At the same time, when the input and guide images ae same guided filter exhibit structural inconsistencies, these existing filters function poorly. Here, we illustrate that these limitations are caused by the guided filter acting as a variable-strength locally isotropic filter on the image. The use of unweighted averaging in the final steps of guided filter variants such as the adaptive guided filter, weighted guided image filter, and gradient-domain guided image filter causes this behaviour, according to our analysis. The Anisotropic Guided Filter (AnisGF) is a novel filter that uses weighted averaging to achieve maximum diffusion while maintaining strong edges in the image. The proposed weights are optimized based on local neighbourhood variances to produce strong anisotropic filtering while maintaining the original guided filter's low computing cost. The proposed method tackles the presence of detail halos and the management of inconsistent structures found in previous guided filter variations, according to s4ynthetic experiments. Furthermore, experiments with sand-dust image enhancement and strip-noise removal also show how the technique improves image quality.

1. INTRODUCTION

1.1 Image Processing

An image can be referred to as a physical representation or likeliness of a person, animal or thing, painted, sculptured, photographed, or otherwise made visible. An image is represented by its dimensions (width and height) determined by the number of pixels. The pixel is a point on the image that takes on a specific shade, color, or opacity, it can be represented either in grayscale, RGB, or RGBA.

Image Processing is a technique of performing operations on an image to enhance the image or extract relevant information from it. Image processing is a type of signal processing where the input is

an image, and the output is either that image or its characteristics or features. Image processing methods can be broadly classified into analog image processing and digital image processing. Hard copies, such as printouts and photographs, can be benefited from analog image processing. Digital image processing techniques aid in the manipulation of digital images through the use of computers. Pre-processing, enhancement, and information extraction are the three general phases that all types of data must go through while using digital techniques. Image processing types can be classified as visualization, recognition, sharpening and restoration, pattern recognition, and retrieval.

The fundamental image processing steps include image acquisition, image enhancement image restoration, color image processing, wavelets and multiresolution processing compression, morphological processing, representation and description, and recognition. With the advancement of technology, digital image processing applications are finding their way into almost every field, including the medical field, image polishing and restoration, UV sensing, transmission and encoding, robot vision, pattern recognition, face detection, and so on.

Image filtering is a fundamental operation in image processing that can significantly improve image quality and yield information. Filtering is the process of replacing the pixel value with the values based on the operations/functions. The operation/functions used on the original image are called filters. Filtering techniques are used to enhance and modify digital images. Also, image filters are used for blurring and noise reduction, sharpening, and edge detection. Image filters are primarily used for suppressing high frequencies for smoothing techniques and low frequencies for image enhancement and edge detection. Images can be filtered in either the frequency domain or the spatial domain. Frequency filtering is based on the process of converting the image to the frequency domain, multiplying it by the frequency filter function, and then re-transforming the result back to the spatial domain. The filter function is designed to attenuate some frequencies and enhance others. The traditional method of image filtering is spatial domain filtering, it is used directly on the image pixels. The process in the spatial domain is to convolve the input image with the filter function.

Based on linearity, spatial domain filters can be classified into linear and non-linear filters. Non-linear filters are used to detect edges. Non-linear filtering techniques are more effective than linear filters. Image details and edges tend to blur in linear image processing. Gaussian filter, Laplacian filter, and neighbourhood Average (Mean) filter can be identified as examples of linear filters. Median filters are non-linear filters.

1.2 Edge Preserving Filter

Edge is a common image feature that can help with feature description, pattern recognition, picture segmentation, image restoration, object tracking, and image compression. Edges are the typical noticeable differences in image intensity level that occur between the boundaries of two different objects in an image. Edge detection is the procedure for determining the borders of objects inside a picture. Edge detection is used to characterize the borders of objects in a scene by detecting abrupt changes in pixel intensity or brightness discontinuities.

Several edge detection methods have been implemented, which can be divided into three domains: frequency domain, spatial domain, and wavelet domain. In the frequency domain, an image is converted into the frequency domain and later various operations are performed on it. Phase congruency is a good frequency-domain method to determine the edge information as it utilizes the phase coherence property of the principle moment components. In the spatial domain, on image pixels, gradient operations are directly performed. Here Roberts, Prewitt, and Sobel edge detectors are first-order type methods, where edge detector searches for points where the gradient value is large. Laplacian, Gaussian-Laplacian, and Canny are second-order type methods, where edge detector finds for points where zero-crossings occur. In the wavelet domain, for noise suppression to find improved edge detection, an image is transformed into sub-banded multifrequency levels [68]. The image contour is extracted in high frequencies and fine details are extracted in low frequencies. In contour detection, the multiresolution analysis finds importance. In the Active Shape Model (ASM), the detection of the edges or contours of an object is done by searching for the optimal location of the ASM points based on Principal Component Analysis (PCA) of the gray values at each point on the boundary of the object by the distance minimization procedure.

Traditional edge detector operators such as the Sobel operator, Robert operator, and Prewitt operator are simple to detect edges along with their orientations and are easy to implement. Zero-crossing operators such as the Laplacian and other second derivative operators have globally fixed properties concerning the detection of edges. But all of these operators are sensitive to noise. On the other hand, in noisy conditions, the canny operator detects better edges as it accommodates a method to counter noise problems before edge detection. Smith and Brady implemented non-derivative filtering named SUSAN, which can suppress noise and detect edges in a faster way.

With all the edge detection techniques, a clear threshold or demarcation is required between the pixels with significant local intensity variations (i.e. edge pixels) and non-significant local intensity variations (i.e. non-edge pixels). However, noise is always an issue at this boundary. To select the threshold, the false alarm error probability, when detecting the edge pixels must be minimum. To handle this, researchers have adopted fuzzy reasoning to successfully detect edge strength without being misled by noise. Later, to find the exact edges researchers moved to evolutionary optimization algorithms, such as particle swarm optimization (PSO), bacterial foraging algorithm (BFA), genetic algorithm (GA), bee colony optimization (BCO), etc. to find the optimum threshold.

2.Existing Methods

2.1 Guided filtering

The guided filter, proposed in [1], performs filtering via concept shape transformations [12] on an image locally. It is feasible to arrange the pixel values into a vector y_i given a patch from the input image referenced with the subscript i. This patch vectorises to q_i and corresponds to another patch taken from the same position of the guide image. The guided filter is then given the task of determining a pair of scalar values, s_i and t_i, that solve the following problem:

$$\underset{a_i,b_i}{\operatorname{argmin}} \frac{1}{n}\|y_i - (s_i q_i + t_i)\|_2^2 + \gamma |s_i|_2^2 \tag{1}$$

where n denotes the number of pixels in the patch and γ is a small regularisation constant that prevents s_i from being too large. The variable s_i serves as a scaling factor for detail transference, whereas t_i serves as a bias factor for patch intensity adjustment. This formula yields the following closed form solution:

$$a_i = \frac{\frac{1}{n}(x_i - \bar{x}_i)^T (g_i - \bar{g}_i)}{\frac{1}{n}(g_i - \bar{g}_i)^T (g_i - \bar{g}_i) + \gamma}$$

$$= \frac{\operatorname{cov}(x_i - \bar{x}_i, g_i - \bar{g}_i)}{\operatorname{var}(g_i - \bar{g}_i) + \gamma} \tag{2}$$

$$t_i = \bar{y}_i - s_i \bar{q}_i \tag{3}$$

The patch meanings are represented by $\bar{y}_i$ and $\bar{q}_i$.

In vector space, the operation of the guided filter can be divided into two parts. By subtracting the patch means from both patches, the resulting vectors $\tilde{x} = x - \bar{x}$ and $\tilde{g} = g - \bar{g}$ reside in hyperplane orthogonal to the ones vector 1 = [1, 1, · · · , 1]. The scalar projection of $\tilde{y}$ on $\tilde{q}$, assuming an infinitesimal γ, is described by the parameter $\check{s}$ within this hyperplane. The patch as a result of this transformation:

$$\hat{y}_i = s_i q_i + t_i \tag{4}$$

$$= s_i(q_i - \bar{q}_i + \bar{q}_i) + (\bar{y}_i - s_i \bar{q}_i)$$

$$\hat{y}_i = s_i \tilde{q}_i + \bar{y}_i \tag{5}$$

specifies a resultant vector that has a constant magnitude along the 1 vector and a variable value along the orthogonal $\tilde{g}$ vector. This magnitude, as commanded by a_i, is controlled only by the γ parameter in the guided filter, and is bounded as $a_i \leq \check{a}_i$ when $\gamma \to 0$ The guided filter's vector perspective makes it easier to visualise diffusion processes.

2.2. Guided Filtering as Diffusion Process

In classical diffusion, particles of varied densities spread throughout space freely redistribute over time according to the diffusion equation. This process will continue until the particles achieve a state of balance. When diffusion occurs within a closed container, this equilibrium occurs when all particles are spread evenly. Some of the process key qualities are as follows:
1) The average particle density within the container remains constant due to the constant number of particles inside.
2) Because diffusion moves particles from higher density regions to lower density regions, the local densities will never be lower than the initial minimum density or higher than the initial maximum density.

The concept of particle density in photographs corresponds to pixel intensities. Nonetheless, image diffusion will follow the two properties described above. With this new perspective on diffusion, the issue arises: Can the directed filter be considered a diffusion process? Discrete isotropic diffusion is technically equivalent to a Gaussian kernel, although it differs significantly from the guided filter kernel. Looking at the guided filter from the vector perspective, however, reveals the following:
1) The component $\bar{x}_i 1$ is constant in the resultant vector and orthogonal to the structural vector $\tilde{g}_i$ meaning that the mean of the transformed patch is constant regardless of the value of a_i.
2) The largest structural information transfer occurs when the vector projection with γ approaches zero. Regularizing γ will reduces the amount of detail in the resulting patch, so filtering can only reduce the magnitude of the structural vector, keeping the minimum and maximum intensity constraints.

While the guided filter is not an exact diffusion process based on these two characteristics, it acts similarly. In this diffusive approach, the factor ai effectively correlates to the degree of diffusion. On a patch level, the guided filter behaves isotropically, which is a more subtle feature. The diffusion process does not favour any one pixel in the locality since the effect of ai is limited to the vector g. Instead, the guided filter evenly distributes all structural information within the patch, regardless of geographical distance.

2.3. Image-level Diffusion

On a patch level, the guided filter's approximate diffusive behavior is applicable. On the other hand, multiple overlapping patches can change a single pixel in an image. As a result, the initial guided filter takes into consideration the average effect:

$$\bar{s}_i = \frac{1}{n}\sum_{j\in N(i)} s_j \qquad (6)$$

where N(i) denotes the neighborhood around pixel i. Because s differs for each patch, it is spatially variable, and the resulting averages are also spatially variable. The resulting filter is region-selective and anisotropic, but only to a limited extent.

Consider the one-dimensional synthetic signal to even further understand this. To show the effect of the guided filter, this signal is filtered with a 33-point guided filter after adding Gaussian noise. The filtered signal shows that the filtering power appears to be weaker near the edges, causing the appearance of noise to be more evident in these areas. A thorough examination of the scaling factor enables us to more easily understand this phenomenon. However, because this example is self-guided (i.e. the input signal is utilized as the guide signal), the ideal scalar projection $\check{a}_i$ for all sections of the signal is equal to 1. When the regularization constant is considered, the following declaration emerges:

$$s_i = \frac{\mathrm{var}(y_i - \bar{y}_i)}{\mathrm{var}(y_i - \bar{y}_i) + \gamma} = \frac{\sigma_i^2}{\sigma_i^2 + \gamma} \qquad (7)$$

where σ_i is the local variance of neighborhood i. Which means that for detailed regions (i.e. bigger variations), the scaling factor is closer to 1 and for smoother regions it is closer to 0. his regularization has the advantage of keeping the signal's detailed regions strong while aggressively dispersing portions with less information. With this in mind, a closer examination of the patch-level scaling factors ai in Fig. 2d indicates that they are nearly bilevel. The filter prioritizes structure transfer ($s \to 1$) towards the central structure, while smoothing ($s \to 0$) is preferred for the side areas. At points

24 and 77 of the signal, which correspond to the limits of the 33-point region unaffected by the centre structure, clear transitions arise. This means that the side portions of the patch should be smoothed out. The average scaling factors, which are also displayed in Fig. 2d, operate as a low-pass filter, smoothing out the scaling factors. As a result, the amount of detail kept around the edges tapers off into a smooth transition, resulting in an artefact called as a "detail halo" in this work. This effect is most noticeable when using the guided filter with large window sizes, although it may also be seen with photos. Returning to the previous point, the final scaling factors a_i are anisotropic, meaning that diffusion is stronger in some areas. However, its behaviour is only slightly anisotropic. The effect of averaging imposes a low-pass filter on the final scaling components, effectively eliminating the filter's aggressive anisotropic capabilities. When using bigger neighborhood sizes, the low-pass filtering effect is amplified, resulting in higher detail halo artefacts. The AGF [14], the WGIF [5], and the GGIF [46] are all weakly anisotropic since they all use the same simple averaging step of the guided filter.

2.4. Inconsistent Structures in the Guided Filter

Aside from the detail halo issue, the guided filter's poor performance when dealing with inconsistent structures is another downside (For example, when the input and guide patches are structured differently). Despite the fact that [60] solved the problem, their proposed method is iterative and computationally expensive, leaving room for improvement. Consider the identical signal, but with a step function as the guiding function to find the source of the problem. Other filtering techniques, such as WLS and WL1, employ the guiding image's gradient map to produce filtering, which effectively compels smoothing to occur only in the parts of the input image matching to the step function's flat regions, while respecting the high-gradient border at point 50.

This is certainly not the case with the guided filter. In terms of the scaling factors s_i and $\bar{s}_i$, there is almost no structural relationship between the two signals in. These conditions provide a nearly isotropic behaviour in which all $\bar{a}_i$ approaches 0. This near-isotropic behaviour also allows structural information from the input image to cross the high-gradient boundary of the guiding function. When dealing with inconsistent structures, the guided filter fails due to a lack of anisotropy.

2.5. Weighted Guided Image Filter

This section proposes an edge-aware weighting, which is then merged into the GIF in [14] to generate the WGIF.

An Edge-Aware Weighting

Let G represent a guidance image and, $\sigma^2_{G,1}(p')$ represent G's variance in the 3×3 window, $\Omega_1(p')$. Using local variances of 3×3 windows of all pixels, an edge-aware weighting $\Gamma_G(p')$ is defined as follows:

$$\Gamma_G(p') = \frac{1}{N}\sum_{p=1}^{N} \frac{\sigma^2_{G,1}(p')+\varepsilon}{\sigma^2_{G,1}(p)+\varepsilon} \quad (8)$$

where ε is a tiny constant, whose value is chosen as $(0.001 \times L)^2$, and L is the input image's dynamic range. In the computation of $\Gamma_G(p')$, all pixels in the guidance image are utilised. Furthermore, the weighting $\Gamma_G(p')$determines the relative value of pixel p' to the entire guiding image. For an image with N pixels, the complexity of $\Gamma_G(p')$ is $O(N)$ due to the box filter.

When p' is at an edge, $\Gamma_G(p')$ is usually greater than 1, and when p' is in a smooth area, G(p) is usually smaller than 1. The weighting $\Gamma_G(p')$ in equation clearly assigns bigger weights to pixels at edges than to pixels in flat areas. There may be blocking artefacts in final photos after applying this edge-aware weighting. A Gaussian filter smooths the value of $\Gamma_G(p')$ to prevent blocking artefacts from appearing in the final image. Pixels at the borders are clearly given higher weights than pixels in flat areas. The proposed weighting corresponds to a property of the human visual system, namely that pixels near sharp edges are frequently more essential than those in flat areas. It should be noted that the proposed weighting $\Gamma_G(p')$ is only one type of edge-aware weighting; there are many others, including those derived from the Sobel and Roberts gradients. By introducing edge-aware weighting into the GIF, it can be improved. The proposed weighting $\Gamma_G(p')$, is used as an example in the next section to demonstrate the WGIF.

3. PROPOSED METHOD

3.1 Anisotropic Guided Filtering

Both limitations share the lack of anisotropy in the formulation of current guided filters. The problem of detail haloing, which we mentioned before, reveals that these filters are only weakly anisotropic. While the averaging step accurately adjusts the level of diffusion to preserve strong edges, low-pass filtering these values completely eliminates these measures. When is low, this process preserves detail at an edge due to weak diffusion, whereas when is large, it erodes the edge due to excessive diffusion.

Existing guided filters don't follow the gradient restrictions of the guide picture when dealing with inconsistent structures because they lack anisotropy. The WLS and WL1 global filters employ a penalty term based on the gradients of the guide image. By preventing the filter from bridging large gradients in the guiding picture, this penalty causes an anisotropic effect. The covariance of the input and guide patches affects the diffusion effect in guided filters. When structures are inconsistent, the covariances are modest, resulting in small a i values, which permit strong diffusion while ignoring the gradient restrictions in the guide patch. Anisotropic integration, similar to detail halos, can be used to eliminate this. This, like detail halos, can be avoided by including anisotropy in the filter formulation, particularly one derived from the structure of the guiding picture. The regularisation of a i has little to no effect on the degree of anisotropy in each of these situations due to the final averaging step used in each. This suggests that normal guided filter versions like AGF, WGIF, and GGIF have the same concerns. We can improve anisotropy by regularising the averaging step rather than regularising a i. As a result, we recommend using a weighted average strategy:

$$\tilde{s}_i = \sum_{j \in N(i)} \omega_{ij} s_j \quad (8)$$

$$\tilde{t}_i = \sum_{j \in N(i)} \omega_{ij} t_j \quad (9)$$

where ij is the weight given to a pixel in a neighbourhood at j that surrounds the central pixel at i. The goal of these weights is to maximise diffusion while keeping the guide image's edge boundaries strong. This isn't the first time a weighted averaging method has been used to tweak the guided filter. The demos icing technique employs a residual variance-based weighted averaging algorithm. Because its function was to communicate detail between colour channels in an image, it was designed to minimise the transformation error of the guided patch to the input patch. Due to the residual variance requirements, any structural differences between the two patches are discarded in favour of a transformation that attempts to rebuild the input patch as closely as possible while avoiding diffusion effects.

4.RESULTS AND DISCUSSIONS

Anisotropic Guided Filter

Fig. 1a Input Image

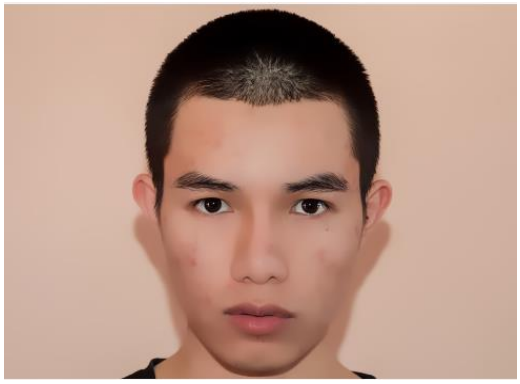

Fig. 1b Output Image

Fig. 2a Input Image

Fig. 2b Output Image

Experiment results show that the output image strongly adheres to the input image's gradient structure. The anisotropic guided filter is smoothing-oriented which has complexity of O(n).

	Input Image	Output Image
PSNR	13.5577	23.6477
SSID	0.7361	0.7461

Table 1: PSNR and SSID values for fig 1a, fig 1b

	Input Image	Output Image
PSNR	19.8039	27.5594
SSID	0.6642	0.7899

Table 2: PSNR and SSID values for fig 2a, fig 2b

Sand-Dust Image Enhancement using Anisotropic Guided Filtering

Fig. 3a Input Image

Fig. 3b Output Image using GF

Fig. 3c Output Image using AnisGF

The process of image enhancement here includes three components in sequence: Color Correction in the LAB color space based on gray world theory, Dust Removal using a halo-reduced DCP dehazing method, and Contrast Stretching in the LAB color space using a Gamma function improved contrast limited adaptive histogram equalization (CLAHE), in which a guided filter is used to improve the artifacts of the histogram equalization.

	Input Image	Output Image using GF	Output Image using AnisGF
PSNR	13.9743	14.2029	18.9883
SSID	0.7973	0.8125	0.9444

Table 3: PSNR and SSID values for fig. 3a, 3b, 3c

Noise Removal Using Anisotropic Guided Filter

Salt-pepper noise removal

Fig. 4a Input Image

Fig. 4b Output Image

The salt-pepper noise removal is based on denoising method that exploits the relationship between pixel's values when the image changes color. which gives ordered sequences of values in the four directions, horizontal, vertical and diagonals of the window. The method relays on this concept to change the corrupted pixel, by using the neighbors in the window to extracts the truest value (subjects to this sequence) of the treated pixel.

	Input Image	Output Image
PSNR	15.9512	17.5725
SSID	0.4845	0.7529

Table 4: PSNR and SSID values for fig. 4a,4b

Infrared Strip-Noise Removal Using Anisotropic Guided Filter

Fig. 5a Input Image

Fig. 5b Output Image usin g GF

Fig. 5c Output Image using AnisGF

The algorithm accurately removes strip-type noise present in infrared images without causing blurring effects. Firstly, a 1D row guided filter is applied to perform edge-preserving image smoothing in the horizontal direction. The extracted high-frequency image part contains both strip noise and significant amount of image details. Through a thermal calibration experiment. Based on the derived strip noise behavioural model, strip noise components are accurately decomposed from the extracted high-frequency signals by applying 1D column guided filter. Finally, the estimated noise terms are subtracted from raw infrared images to remove strips without blurring image details.

	Input Image	Output Image Using GF	Output Image using AnisGF
PSNR	17.7315	18.0575	24.4497
SSID	0.3668	0.4811	0.7584

Table 5: PSNR and SSID values for fig. 5a,5b,5c

4.CONCLUSION AND SCOPE OF FUTURE WORK

Conclusion

This study developed a novel filter that builds on the guided filter's foundation while addressing many of its drawbacks. AnisGF can simply be considered of as a generalised guided filter. This can be parameterized to reproduce the behaviour exactly of the latter. This characteristic suggests that new filter may be used in the numerous applications that already avail, while adding anisotropy into the guided filter's performance as an additional capacity This anisotropic behaviour could be ubiquitous. This anisotropic behaviour may be more desirable in some applications such as enhancement, noise

reduction and segmentation. As identified in this work, the AnisGF still presents some limitations, particularly with density dependence which can be addressed by extending the filter to multiple scales.

Scope of Future Work

The Gaussian Spatial weighing can replace the regularization term. With the use of Adaptive Regularization term, instead of dependence on local variance we can allow for the reuse of already computed values. Further advancement in the algorithm can be introduced by Deep Convolution Neural Network.

5.REFERENCES

[1] Kaiming He, Jian Sun, and Xiaoou Tang, "Guided Image Filtering", IEEE transactions on Pattern Analysis and Machine Intelligence, 2013.
[2] P. Perona and J. Malik, "Scale-Space and Edge Detection Using Anisotropic Diffusion," IEEE Trans. Pattern Analysis and Machine Intelligence, July 1990.
[3] Z. Farbman, R. Fattal, D. Lischinski, and R. Szeliski, "Edge conserving Decompositions for Multi-Scale Tone and Detail Manipulation," Proc. ACM Siggraph, 2008.
[4] J. G. Harris and Y.-M. Chiang, "Nonuniformity correction of infrared image sequences using the constant-statistics constraint," Image Processing, IEEE Transactions on, vol. 8, no. 8, pp. 114, 1999.
[5] Zhengguo Li, Jinghong Zheng, Member, Zijian Zhu, Wei Yao, Shiqian Wu, "Weighted Guided Image Filtering," IEEE transactions on image processing, January 2015.
[6] Harbonnier, L. Blanc-Feraud, G. Aubert, and M. Barlaud, "Deterministic edge-preserving regularization in computed imaging," IEEE Transactions on Image Processing, Feb. 1997.
[7] Z. G. Li, J. H. Zheng, and S. Rahardja, "Detail-enhanced exposure fusion," IEEE Transactions on Image Processing, Nov. 2012.
[8] K. He, J. Sun, and X. Tang, "Single image haze removal using dark channel prior," IEEE Trans. Pattern Analysis and Machine Intelligence, Dec. 2011.
[9] C. Tomasi and R. Manduchi, "Bilateral filtering for gray and color images," in Proc. IEEE Int. Conf. Comput. Vis., Jan. 1998.
[10] B. Y. Zhang and J. P. Allebach, "Adaptive bilateral filter for sharpness enhancement and noise removal," IEEE Transactions on Image Processing, May 2008.
[11]. A. Averbuch, G. Liron, and B. Z. Bobrovsky, "Scene based nonuniformity correction in thermal images using kalman filter," Image and Vision Computing, vol. 25, no. 6, pp. 833–851, 2007
[12] D. R. Pipa, E. A. da Silva, C. L. Pagliari, and P. S. Diniz, "Recursive algorithms for bias and gain nonuniformity correction in infrared videos," Image Processing, IEEE Transactions on, vol. 21, no. 12, pp. 4758–4769, 2012
[13] K. He, J. Sun, and X. Tang, "Guided image filtering," in Computer Vision–ECCV 2010. Springer, 2010, pp. 1–14.
[14] C. C. Pham, S. V. U. Ha, and J. W. Jeon, "Adaptive guided image filtering for sharpness enhancement and noise reduction," in Advances in Image and Video Technology. Berlin, Germany: Springer-Verlag, 2012.
[15] Ruturaj G. Gavaskar and Kunal N. Chaudhury, "Fast Adaptive Bilateral Filtering," IEEE Transactions on Image Processing, Feb 2019.
[16] Danny Barash," A Fundamental Relationship Between Bilateral Filtering,Adaptive Smoothing, and the Nonlinear Diffusion Equation". IEEE Transactions on Pattern Analysis and Machine Intelligence June 2002
[17] S. Paris, and F. Durand, "A fast approximation of the bilateral filter using a signal processing approach," 9th European Conference Computer Vision (ECCV) 2006
[18] Bo-Hao Chen, Yi-Syuan Tseng, and Jia-Li Yin, "Gaussian-Adaptive Bilateral Filter," IEEE Signal Processing Letters, 2020
[19] Zenglin Shi, Yunlu Chen, Efstratios Gavves, Pascal Mettes, Cees G. M. Snoek, "Unsharp mask guided filtering," IEEE transactions on Image Processing, 2021.
[20] F. Kou, W. Chen, C. Wen, and Z. Li, "Gradient-domain guided image filtering," IEEE Trans. Image Process, Nov. 2015.
[21] Z. Sun, B. Han, J. Li, J. Zhang, and X. Gao, "Weighted guided image filtering with steering kernel," IEEE Trans. Image Process, 2020

[22] B. Albahar and J.-B. Huang, "Guided image-to-image translation with bi-directional feature transformation," in Proc. IEEE/CVF Int. Conf. Comput. Vis. (ICCV), Oct. 2019
[23] H. Su, V. Jampani, D. Sun, O. Gallo, E. Learned-Miller, and J. Kautz, "Pixel-adaptive convolutional neural networks," in Proc. IEEE/CVF Conf. Comput. Vis. Pattern Recognit. (CVPR), Jun. 2019
[24] Y. Li, J.-B. Huang, N. Ahuja, and M.-H. Yang, "Joint image filtering with deep convolutional networks," IEEE Trans. Pattern Anal. Mach, Aug. 2019.
[25] Y. Li, J.-B. Huang, N. Ahuja, and M.-H. Yang, "Deep joint image filtering," in Proc. ECCV, 2016
[26] T.-W. Hui, C. C. Loy, and X. Tang, "Depth map super-resolution by deep multi-scale guidance," in Proc. ECCV, 2016, pp.
[27] Pan, J. Dong, J. S. Ren, L. Lin, J. Tang, and M.-H. Yang, "Spatially variant linear representation models for joint filtering," in Proc. IEEE/CVF Conf. Comput. Vis. Pattern Recognit. (CVPR), Jun. 2019.
[28] A. Hosni, C. Rhemann, M. Bleyer, C. Rother, and M. Gelautz, "Fast cost-volume filtering for visual correspondence and beyond," IEEE Transactions on Pattern Analysis and Machine Intelligence, vol. 35, no. 2, pp. 504–511, Feb. 2013
[29] Polesel, A., Ramponi, G., Mathews, V.G.: Image Enhancement via Adaptive Unsharp Masking. IEEE Trans. Image Processing 2000
[30] A. Buades, B. Coll, and J.-M. Morel, "A non-local algorithm for image denoising," in Computer Vision and Pattern Recognition, 2005. CVPR 2005. IEEE Computer Society Conference on, vol. 2. IEEE, 2005, pp. 60–65.
[31] Kim and J. P. Allebach, "Optimal unsharp mask for image sharpening and noise removal," J. Electron. Imag., vol. 14, 2005.
[32] K. Dabov, A. Foi, V. Katkovnik, and K. Egiazarian, "Image denoising by sparse 3D transform-domain collaborative filtering," Image Processing, IEEE Transactions on, vol. 16, no. 8, pp. 2080–2095, 2007
[33] G. R. Arce and R. E. Foster, "Detail-preserving ranked-order based filters for image processing," IEEE Trans. Acoust., Speech, Signal Process, Jan 1989.
[34] O. V. Michailovich, "An Iterative Shrinkage Approach to Total-Variation Image Restoration, IEEE Trans. on Image Processing, May 2011.
[35] M. Elad, "On the origin of the bilateral filter and the ways to improve it," IEEE Trans. Image Process, Oct 2002.
[36] D. Barash, "A fundamental relationship between bilateral filtering, adaptive smoothing, and the nonlinear diffusion equation," IEEE Trans. Pattern Anal. Mach. Intell, Jun. 2002.
[37] Z. Farbman, R. Fattal, D. Lischinshi, and R. Szeliski, "Edge-preserving decompositions for multi-scale tone and details manipulation", ACM Trans. on Graphics, Aug. 2008.
[38] P. Perona and J. Malik, "Scale-space and edge detection using anisotropic diffusion," IEEE Trans. Pattern Anal. Mach. Intell Jul 1990.
[39] M. J. Black, G. Sapiro, D. H. Marimont, and D. Heeger, "Robust anisotropic diffusion," IEEE Trans. Image Process, Mar 1998.
[40] N. J. Morris, S. Avidan, W. Matusik, and H. Pfister, "Statistics of infrared images," in Computer Vision and Pattern Recognition, 2007. CVPR'07. IEEE Conference on. IEEE, 2007, pp. 1–7
[41] L. Yin, R. Yang, M. Gabbouj, and Y. Neuvo, "Weighted median filters: a tutorial,", IEEE Trans. on Circuits and Systems II: Analog and Digital Signal Processing, 1996.
[42] Z. Ma, K. He, Y. Wei, J. Sun, and E. Wu, "Constant time weighted median filtering for stereo matching and beyond," in 2013 IEEE International Conference on Computer Vision (ICCV), Dec 2013, Australia.
[43] J. Zhao, Q. Zhou, Y. Chen, T. Liu, H. Feng, Z. Xu, and Q. Li, "Single image stripe nonuniformity correction with gradient-constrained optimization model for infrared focal plane arrays," Optics Communications, vol. 296, pp. 47–52, 2013
[44] S. Guillon, P. Baylou, M. Najim, and N. Keskes, "Adaptive nonlinear filters for 2D and 3D image enhancement," Signal Process, 1998
[45] Y. Cao and Y. Li, "Strip non-uniformity correction in uncooled longwave infrared focal plane array based on noise source characterization," Optics Communications, vol. 339, pp. 236–242, 2015.
[46] A. Levin, D. Lischinski, and Y. Weiss, "A closed-form solution to natural image matting," IEEE Transactions on Pattern Analysis and Machine Intelligence, Feb 2008.
[47] S. Li, X. Kang, and J. Hu, "Image fusion with guided filtering," IEEE Transactions on Image Processing, Jul 2013.
[48] B. Ham, D. Min, and K. Sohn, "A generalized random walk with restart and its application in depth up-sampling and interactive segmentation," IEEE Transactions on Image Processing, Jul. 2013.
[49] Z. Ma, K. He, Y. Wei, J. Sun, and E. Wu, "Constant time-weighted median filtering for stereo matching and beyond," in 2013 IEEE International Conference on Computer Vision. IEEE, Dec. 2013.

[50] Q. Zhu, J. Mai, and L. Shao, “A fast single image haze removal algorithm using color attenuation prior,” IEEE Transactions on Image Processing, Nov 2015.
[51] -Y. Kim, L.-S. Kim, and S.-H. HWang, ‘‘ An advanced contrast enhancement using partially overlapped sub-block histogram equalization,’’ IEEE Trans. Circuits Syst. Video Technol., vol. 11, no. 4, pp. 475–484, Apr. 2001.
[52] D. Kiku, Y. Monno, M. Tanaka, and M. Okutomi, “Beyond color difference: Residual interpolation for color image demosaicking,” IEEE Transactions on Image Processing, 2016
[53] J. Weickert, B. Romeny, and M. Viergever, “Efficient and reliable schemes for nonlinear diffusion filtering,” IEEE Transactions on Image Processing, Mar. 1998.
[54] J. Wang, Y. Pang, Y. He, and C. Liu, ‘‘Enhancement for dust-sand storm images,’’ in Proc. 22nd Int. Conf. Multimedia Model., New York, NY, USA, 2016, pp. 842–849.
[55] Y. Kim, D. Min, B. Ham, and K. Sohn, “Fast domain decomposition for global image smoothing,” IEEE Transactions on Image Processing, Aug. 2017.
[56] Carlo Noel Ochotorena, Yukihiko Yamashita, “Anisotropic Guided Filtering,” IEEE Transaction on Image Processing, no.1, Sept. 2019.
[57] L. Karacan, E Erdem, and A. Erdem, “Structure-preserving image smoothing via region covariances”. in ACM Trans. on Graphics 2013.
[58] L. Xu, Q. Yan, Y. Xia, and J. Jia, “Structure extraction from texture via relative total variation,” ACM Trans. on Graphics, Nov. 2012.
[59] K. J. Yoon and I. S. Kweon, “Adaptive support-weight approach for correspondence search,” IEEE Trans. on Pattern Analysis and Machine Intelligence, Feb. 2006.
[60] . Zhi, S. J. Mao, and M. Li, ‘‘Visibility restoration algorithm of dustdegraded images,’’ J. Image Graph., vol. 21, no. 12, pp. 1585–1592, Nov. 2016.
[61] C. O. Ancuti, C. Ancuti, C. De Vleeschouwer, and P. Bekaert, ‘‘Color balance and fusion for underwater image enhancement,’’ IEEE Trans. Image Process, Jan. 2018.
[62] Huang, F.-C. Cheng, and Y.-S. Chiu, ‘‘Efficient contrast enhancement using adaptive gamma correction with weighting distribution,’’ IEEE Trans. Image Process., vol. 22, no. 3, pp. 1032–1041, Mar. 2013.